Organic & Biomolecular Chemistry

Enhanced Duplex- and Triplex-forming Ability and Enzymatic Resistance of Oligodeoxynucleotides Modified by a Tricyclic Thymine Derivative

Journal:	*Organic & Biomolecular Chemistry*
Manuscript ID	OB-ART-07-2021-001462.R1
Article Type:	Paper
Date Submitted by the Author:	21-Aug-2021
Complete List of Authors:	Kishimoto, Yuki; Osaka University, Graduate School of Pharmaceutical Sciences Fujii, Akane; Osaka University, Graduate School of Pharmaceutical Sciences Nakagawa, Osamu; Tokushima Bunri University, Faculty of Pharmaceutical Sciences Obika, Satoshi; Osaka University, Graduate School of Pharmaceutical Sciences

ARTICLE

Enhanced Duplex- and Triplex-forming Ability and Enzymatic Resistance of Oligodeoxynucleotides Modified by a Tricyclic Thymine Derivative

Received 00th January 20xx,
Accepted 00th January 20xx

DOI: 10.1039/x0xx00000x

Yuki Kishimoto,[a,b] Akane Fujii,[a,b] Osamu Nakagawa*[a,b,c] and Satoshi Obika*[a,b]

We designed and synthesized an artificial nucleic acid, [3-(1,2-dihydro-2-oxobenzo[*b*][1,8]naphthyridine)]-2′-deoxy-D-ribofuranose (OBN), with a tricyclic structure in a nucleobase as a thymidine analog. Oligodeoxynucleotides (ODNs) containing consecutive OBN displayed improved duplex-forming ability with complementary single-stranded (ss) RNA and triplex-forming ability with double-stranded DNA in comparison with ODNs composed of natural thymidine. OBN-modified ODNs also displayed enhanced enzymatic resistance compared with ODN containing natural thymidine and phosphorothioate modification, respectively, due to the structural steric hindrance of the nucleobase. The fluorescent spectrum of OBN-modified ODNs showed sufficient fluorescence intensity with ssDNA and ssRNA, which are advantageous features for fluorescent imaging techniques of nucleic acids with longer emission wavelengths than bicyclic thymine (bT).

Introduction

Many artificial nucleic acids that are chemically modified on nucleobases, sugar moieties, and phosphodiester linkages have been developed for various applications, such as oligonucleotide therapeutics (antisense[1], antigene[2], small interfering RNA[3], decoy DNA[4], aptamer[5], and CpG oligonucleotide[6]), DNA microarray[7], CRISPR-Cas 9[8], and other purposes. Modification of sugar moieties, which include 2′-fluoro RNA, 2′-*O*-methyl RNA, 2′-*O*-methoxyethyl RNA[9], 2′-aminoethoxy modified derivatives[10], and 2′-*O*,4′-*C*-methylene bridged nucleic acid/locked nucleic acid[11], improve binding affinity (i.e., duplex- or triplex-forming ability)[12] and enzymatic resistance.

In addition to these types of nucleic acid molecules, modification of nucleobases is a fascinating challenge. If Watson-Crick hydrogen bonding sites are retained, the functions of nucleobases can be tailored. Thus, various molecular designs of nucleobases and sugar moieties could be applied. In particular, oligodeoxynucleotides (ODNs) containing modified nucleobases can improve binding affinity by stacking interactions between flanking nucleobases and by retained/altered Watson-Crick base pair patterns, enzymatic resistance, and fluorescent properties because of the expanded ring structure with aromaticity. In fact, size-expanded nucleobase analogs include phenoxazine derivatives, xDNA,[13] yDNA[14], qA derivatives[15], pyrrolo-cytosine derivatives[16], and dioxT[17] were reported. A representative artificial nucleobase with these properties is phenoxazine (tCo)[18] (and G-clamp[19]), a tricyclic cytosine analog (Fig. 1a). tCo- and G-clamp-modified ODNs also feature improved duplex-forming ability and enzymatic stability and become capable of fluorescence. Regarding ODNs

[a] *Graduate School of Pharmaceutical Sciences, Osaka University, 1-6 Yamadaoka, Suita, Osaka 565-0871, Japan, E-mail: obika@phs.osaka-u.ac.jp*
[b] *Core Research for Evolutional Science and Technology (CREST), Japan Sciences and Technology Agency (JST), 7 Gobancho, Chiyoda-ku, Tokyo 102-0076, Japan.*
[c] *Faculty of Pharmaceutical Sciences, Tokushima Bunri University, 180 Nishihamahoji, Yamashiro-cho, Tokushima 770-8514, Japan, osamu_nakagawa@ph.bunri-u.ac.jp*

† Footnotes relating to the title and/or authors should appear here.
Electronic Supplementary Information (ESI) available: [details of any supplementary information available should be included here]. See DOI: 10.1039/x0xx00000x

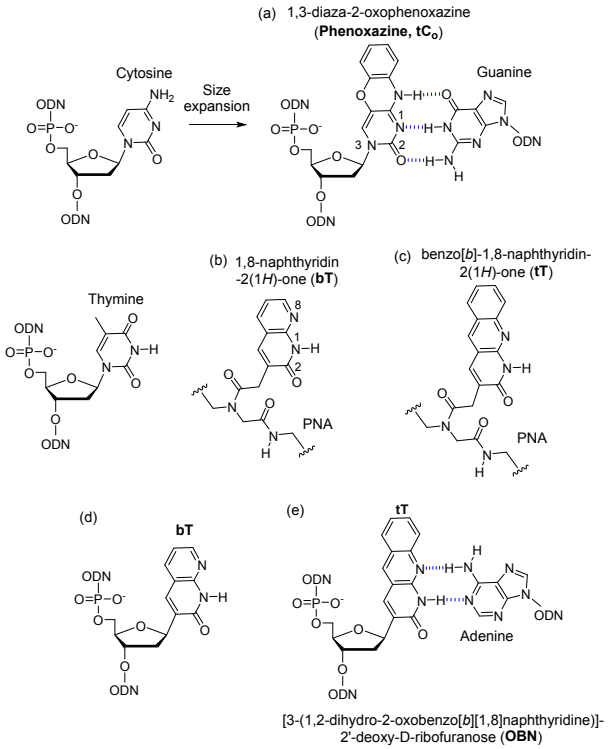

Fig. 1 Structures of multi-cyclic artificial nucleobases.

deoxyribofuranose (dR), many nucleobases are incorporated into the artificial sugar moiety[23], which suggests that the combination of artificial nucleobases and sugar moieties is a plausible strategy.

Focusing on other nucleobases, bi- and tricyclic thymine analogs have been reported. These include 1,8-naphthyridin-2(1*H*)-one (bT) and benzo[*b*]-1,8-naphthyridin-2(1*H*)-one (tT) peptide nucleic acids (PNAs, Fig. 1b, c)[24]. tT-modified PNA (tT-PNA) enhances the duplex-forming ability toward complementary single-stranded (ss) DNA (cDNA), and both bT-PNA and tT-PNA can improve the duplex-forming ability involving ssPNA[24]. Recently, bT was incorporated into the dR (bT-dR); ODNs, including bT-dR, did not significantly change the duplex-forming ability toward cDNA in ODN. Furthermore, ODNs, including bT-dR, were capable of fluorescence (Fig. 1d)[25].

In this study, we designed and synthesized [3-(1,2-dihydro-2-oxobenzo[*b*][1,8]naphthyridine)]-2′-deoxy-D-ribofuranose (OBN) (Fig. 1e). The duplex- and triplex-forming abilities, enzymatic resistance, and fluorescence properties of ODNs modified by OBN were investigated.

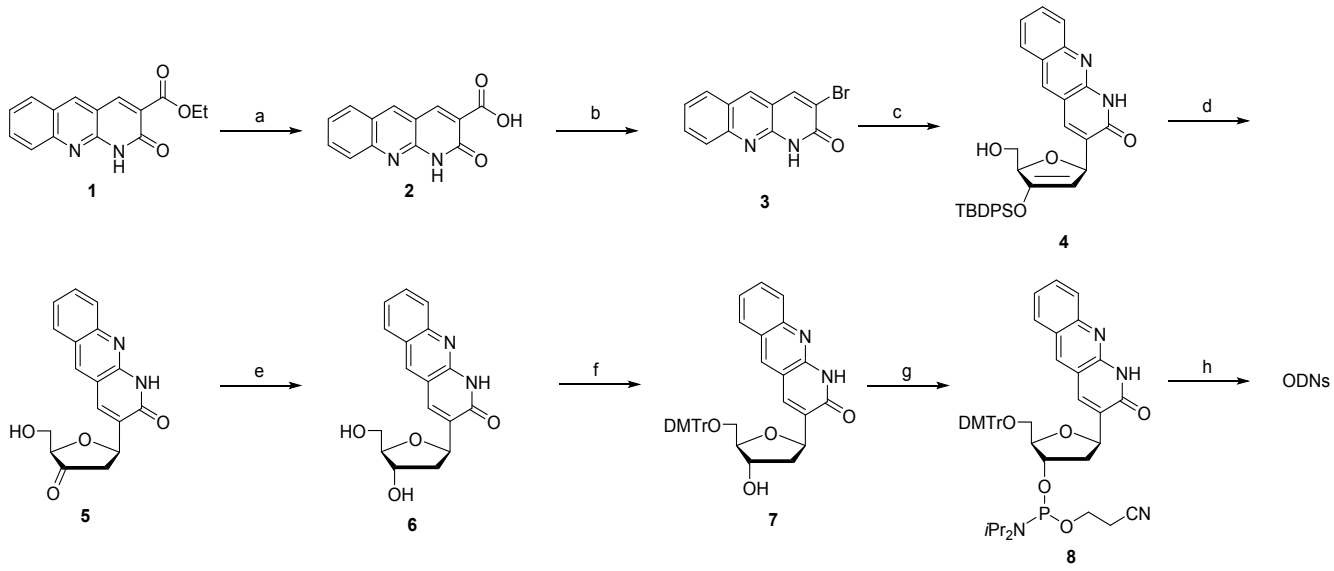

Scheme 1 Synthesis of OBN-modified ODNs.
Reagents and conditions: (a) LiOH, THF/H_2O, 70 °C, 2 h (85%); (b) Br_2, pyridine/DMF, 105 °C, 1 h (81%); (c) 1,4-anhydro-3-*O*-(tertbutyldiphenylsilyl)-2-deoxy-D-erythro-pent-1-entiol, $Pd_2(dba)_3$, P(*o*-tol)$_3$, *n*Bu_3N, 1,4-dioxane, reflux 18 h; (d) TBAF, AcOH, THF, 0 °C, 20 min; (e) $NaBH(OAc)_3$, AcOH, MeCN, -20 °C, 20 min, (23%, three steps); (f) DMTrCl, pyridine, room temperature, 4 h (87%); (g) *i*$Pr_2NP(Cl)OC_2H_4CN$, DIPEA, DCM, room temperature, 3 h, (98%); (h) Automated DNA synthesizer.

bearing G-clamp, especially, 18 °C higher T_m values (T_m values equal to melting temperature) were observed than ODNs composed of natural cytidine instead of the G-clamp. Based on these properties and alteration of nucleobase recognition, many applications of tCo derivatives have been described. These include oligonucleotide therapeutics[20], metal-mediated base pairs[21], and PCR primers[22]. While these nucleobases, as well as tCo or G-clamp, are generally incorporated into

Results and discussion

Synthesis of OBN nucleoside monomer and OBN-modified ODNs

The OBN monomer was synthesized from 1,2-dihydro-2-oxobenzo[*b*][1,8]naphthyridine-3-calboxylate (**1**)[26], which was obtained from acetanilide in five steps (Scheme 1). First, ethyl ester **1** was hydrolyzed to carboxylic acid using lithium hydroxide under tetrahydrofuran in H_2O at 70 °C to produce compound **2**. This

Table 1 T_m values (°C) of duplexes formed between ODNs containing OBN and cDNA or cRNA complement.

Sequence	ODN/cDNA		ODN/cRNA	
	T_m values (ΔT_m/mod.) (°C)	cDNA No.	T_m values (ΔT_m/mod.) (°C)	cRNA No.
ODN**1**: 5′-d(GCGTTTTTTGCT)-3′	40	cDNA**1**	37	cRNA**1**
ODN**2**: 5′-d(GCGTT**B**TTTGCT)-3′	40 (±0)		41 (+4)	
ODN**3**: 5′-d(GCGT**B**T**B**TTGCT)-3′	35 (-2.5)		41 (+2.0)	
ODN**4**: 5′-d(GCGTT**BB**TTGCT)-3′	41 (+0.5)		46 (+4.5)	
ODN**5**: 5′-d(GCG**B**T**B**T**B**TGCT)-3′	27 (-4.3)		35 (-0.7)	
ODN**6**: 5′-d(GCGT**BBB**TTGCT)-3′	44 (+1.3)		51 (+4.7)	
ODN**7**: 5′-d(GCGTCTATTGCT)-3′	40	cDNA**2**	40	cRNA**2**
ODN**8**: 5′-d(GCGTC**B**ATTGCT)-3′	40 (±0)		41 (+1)	
ODN**9**: 5′-d(GCGTCTCTTGCT)-3′	44	cDNA**3**	47	cRNA**3**
ODN**10**: 5′-d(GCGTC**B**CTTGCT)-3′	41 (-3)		48 (+1)	
ODN**11**: 5′-d(GCGTATATTGCT)-3′	36	cDNA**4**	33	cRNA**4**
ODN**12**: 5′-d(GCGTA**B**ATTGCT)-3′	34 (-2)		30 (-3)	
ODN**13**: 5′-d(GCGTGTGTTGCT)-3′	46	cDNA**5**	44	cRNA**5**
ODN**14**: 5′-d(GCGTG**B**GTTGCT)-3′	44 (-2)		40 (-4)	

Conditions: Sodium phosphate buffer (2 mM, pH 7.2) containing 20 mM NaCl. ODNs and cDNA or cRNA (2 μM for each strand) was used. The sequences of each cDNA are 5′-d(AGCAAAAAACGC)-3′ (cDNA**1**), 5′-d(AGCAATAGACGC)-3′ (cDNA**2**), 5′-d(AGCAAGAGACGC)-3′ (cDNA**3**), 5′-d(AGCAATATACGC)-3′ (cDNA**4**), and 5′-d(AGCAACACACGC)-3′ (cDNA**5**) and that of cRNA are 5′-r(AGCAAAAAACGC)-3′ (cRNA**1**), 5′-r(AGCAAUAGACGC)-3′ (cRNA**2**), 5′-r(AGCAAGAGACGC)-3′ (cRNA**3**), 5′-r(AGCAAUAUACGC)-3′ (cRNA**4**), and 5′-r(AGCAACACACGC)-3′ (cRNA**5**). **B** = OBN; ΔT_m/mod. = Change in melting temperature (T_m) value (ΔT_m) per modification relative to the unmodified strand.

compound was brominated by decarboxylation to give **3** under a bromine solution composed of pyridine/*N*,*N*-dimethylformamide (DMF) at 105 °C. Aside from this route, five-membered rings of glycal (1,4-anhydro-3-*O*-(tert-butyldiphenylsilyl)-2-deoxy-D-erythro-pent-1-entiol)[27] were synthesized from acetanilide in five steps. Compound **3** was glycosylated by the Heck reaction utilizing $Pd_2(dba)_3$, P(*o*-tol)$_3$, and *n*-Bu_3N under 1,4-dioxane to yield silylenol ether **4**. The ketone derivative **5** was obtained after the removal of the silyl protecting group by tetrabutylammonium fluoride (TBAF) and stereoselective reduction by sodium triacetoxyborohydride ($NaBH(OAc)_3$). The 5′-hydroxy group of OBN nucleoside **6** was protected by the 4,4′-dimethoxytrityl (DMTr) group in pyridine to produce **7**. The 3′-hydroxy group was phosphorylated to obtain the phosphoramidite unit of OBN (**8**). The molar absorptivity (epsilon at 260 nm) OBN monomer **6** was calculated as 30,000 $L \cdot mol^{-1} \cdot cm^{-1}$ in H_2O containing 0.1% (v/v) dimethylsulfoxide (DMSO) (Fig. S2; Table S1, Supporting Information).

The phosphoramidite unit **8** was successfully incorporated into ODNs utilizing an automated DNA synthesizer under an extended reaction time from 25 s to 2.5 min. The ODNs were cleaved from a controlled pore glass (CPG) column, and their protection groups were removed using 1:1 (v/v) aqueous 28% ammonia/40% methylamine at 65 °C for 10 min. The obtained ODNs were purified by reverse-phase high performance liquid chromatography (RP-HPLC) and identified by matrix-assisted laser desorption/ionization-time of flight mass spectroscopy (MALDI-TOF-MS) (Table S2, Fig. S3 and S4; OBN is designated **B**).

Duplex-forming ability

The binding affinities of the OBN-modified ODNs toward complementary cDNA and cRNA were measured by an ultraviolet (UV) melting experiment that determined the melting temperature (T_m) (Table 1, Fig. S5).

In this experiment, several types of ODNs containing OBN were utilized because it is important for OBN to generate stacking interactions to investigate the selectivity of the flanking nucleobase. Additionally, ΔT_m values were calculated from the differences between each ODN containing OBN and an ODN containing thymidine at the position of OBN. These experiments were conducted using 2 mM sodium phosphate buffer (pH 7.2) containing 20 mM NaCl. The T_m values of ODN**2**/cDNA**1** and /cRNA**1** were 40 °C and 41 °C, respectively. These values were the same (±0 °C) and 4 °C higher than those of unmodified ODN**1**/cDNA**1** and /cRNA**1**, respectively, which were defined as the ΔT_m values. In the duplexes of multiple OBN-modified ODNs and cDNA, alternately modified ODN**3** and **5**/cDNA**1** displayed decreased T_m values compared with ODN**1**/cDNA**1** in response to the increase in the modification [T_m (ΔT_m/mod.): 35 °C (-2.5 °C) and 27 °C (-4.3 °C) each]. In contrast, continuously modified ODN**4** and **6**/cDNA**1** displayed slightly increased T_m values [T_m (ΔT_m /mod.): 41 °C (+0.5 °C) and 44 °C (+1.3 °C), respectively] in response to the increased number of consecutive modifications compared with ODN**1**/cDNA**1**. With regard to the duplexes of OBN-modified ODNs and cRNA, ODN**3** and **5**/cRNA**1** showed suppressed T_m (ΔT_m/mod.) values [41 °C (+2.0 °C) and 35 °C (+0.7 °C), respectively] in contrast with the single modified ODN**2**/cRNA. ODN**4** and **6**/cRNA**1**

displayed increased T_m (ΔT_m/mod.) values compared with ODN**1**/cRNA**1** [46 °C (+4.5 °C) and 51 °C (+4.7 °C), respectively]. T_m (ΔT_m/mod) values of ODN**4** and **6**/cRNA**1** improved with the duplex formation of ODN**4** and **6**/cDNA**1**. Therefore, OBN-modified ODN was able to form a stable duplex with complementary strands, especially cRNA. In both ODN-modified ODN**4** and **6**/cDNA**1** or cRNA**1**, ΔT_m/mod. were higher than those of ODN**2**/cDNA**1** or /cRNA**1** because of consecutive modifications.

Duplexes of singly OBN-modified ODN bearing various flanking nucleobases for OBN and cDNA showed the same or lower T_m values compared to unmodified ODN/cDNA, which were affected by flanking nucleobases of OBN in ODN. T_m values of ODN**2**, **8**, and **10**/cDNA containing pyrimidine base (thymine and cytosine) as adjacent nucleobases of OBN were maintained [40 °C (±0 °C)] or decreased [41 °C (-3 °C)] in relation to ODN**1**, **7**, and **9**/cDNA as T_m (ΔT_m) values. This decreasing tendency of T_m values was observed in ODN**12** and ODN**14**/cDNA (T_m of 34 and 44 °C, respectively). The ΔT_m values of the adjacent purine nucleobases (adenine and guanine) were both decreased by 2 °C compared with ODN**11** and **13**/cDNA. In the duplex formation of ODN**2**, **8**, and **10** containing pyrimidine bases as adjacent nucleobases for OBN toward cRNA, the T_m (ΔT_m) values of ODN**2**, **8**, and **10**/cRNA were 41 °C (+4 °C), 41 °C (+1 °C), and 48 °C (+1 °C), respectively. ODN**12** and **14**/cRNA, including purine base,

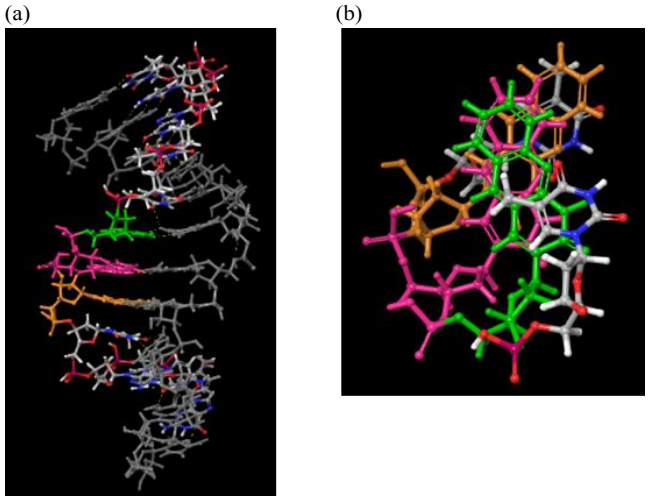

Fig. 2 Snapshots of molecular dynamics (MD) simulations.
MD simulations were conducted using MacroModel software (Schrödinger, LLC) and OPLS3 force field of ODN**6**/cRNA**1** in H_2O at 300 K for 30 ns. The overview is shown in (a) and the op view in (b). Orange, pink, and green molecules indicate each OBN from the 5′-side to the 3′-side in ODN**6**/cRNA**1**.

displayed decreased T_m (ΔT_m) values compared with ODN**11** and **13**/cRNA [30 °C (-3 °C) and 40 °C (-4 °C), respectively]. For stable duplex formation of OBN-modified ODN and cRNA, appropriate sequence design by pyrimidines (especially thymine) at the 5′-side position for OBN was preferred.

Molecular dynamics (MD) simulation for ODN**6**/cRNA**1** indicated that consecutive OBNs stack with each other in the ODN (Fig. 2), which might induce stronger stacking interactions between OBNs compared to thymidine. In addition, hydrogen bonding between OBNs and adenines was retained in the duplex, and the duplex structure was almost maintained because of the OBN incorporation retaining plane base pairs. These results presumably support the enhanced binding affinity of ODN containing consecutive OBN toward cRNA.

Regarding the duplex-forming ability, the contributions of OBN-modified ODNs with tCo-[18b,23a], bT-dR-ODNs[25], and tT-PNA could be compared[24]. We discuss single and multiple modifications in ODN separately. Concerning the single modification in ODN, given that tCo-ODN/cDNA showed higher T_m values than ODNs/cDNA bearing natural cytidine at the tCo position, where the 5′-side adjacent nucleobases of the cytidine are pyrimidines (both cytidine and thymidine), different stacking interaction styles between OBN and tCo would produce differences in their T_m values. In contrast, the observations that OBN-ODN/cRNA increased thermodynamic stability as well as tCo-ODN/cRNA infer that the similarity of the stacking interaction of OBN and tCo in ODN made their results similar.

In addition, it was common that the duplexes of both OBN- and tCo-ODNs /cDNA and /cRNA, where T_m values were decreased when purine nucleobases were incorporated on both the 5′-and 3′-sides of OBN or tCo in the ODNs. T_m values of ODN**10**, **12**, and **14**/cDNA decreased in comparison with bT-dR-modified ODNs bearing the same adjacent nucleobase pattern. This comparison inferred that the benzene ring of OBN was not favorable for the stability of the duplex with cDNA in these sequences. Moreover, considering that T_m values of tT-PNA/cDNA and /cRNA did not change significantly from PNA/cDNA and /cRNA bearing thymine in the tT position, there were no remarkable differences in the stabilization effect of tT when tT was incorporated into PNA. However, while ODN**2**, **8**, and **10**/cDNA decreased or maintained T_m values in comparison with ODN**1**/cDNA, ODN**2**, **8**, and **10**/cRNA increased compared to ODN**1**/cRNA. Thus, when OBN was incorporated into ODNs, cRNA would be a more favorable target than cDNA for OBN-ODNs.

In the multiple modification sequences, OBN-ODNs showed a similar tendency to consecutively modified tCo-ODNs. Regarding duplexes of tT-PNA/cDNA and /cRNA containing consecutive modifications did not change the T_m value. Therefore, consecutive OBNs in ODNs could function in duplex stability more suitably than tT-PNA, differing from a single modification. This result might be attributed to the balance of the strength of the stacking interaction due to OBN and the appropriate rigidity of the furanose. Alternatively, it could contribute to differences in duplex structure between PNA/cDNA or /cRNA and ODN/cDNA or /cRNA.

Mismatch discrimination ability

The mismatch nucleobase discrimination ability of the OBN-modified ODN was evaluated by another UV melting experiment (Table 2, Fig. S6).

Table 2 T_m values (°C) of duplexes formed between ODNs containing **B** and ssDNA or ssRNA complement.

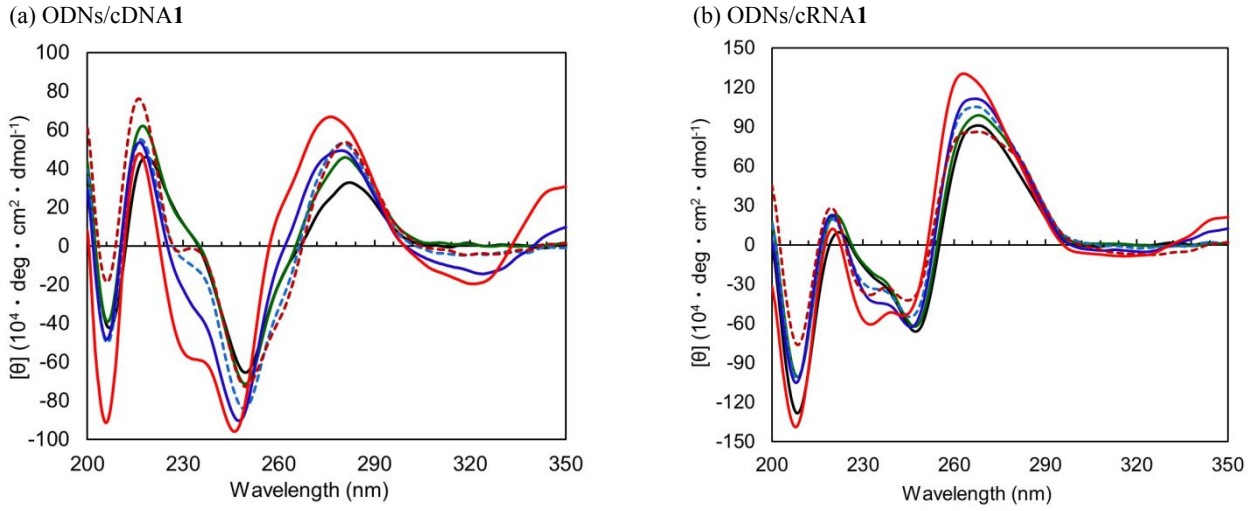

Fig. 3 Circular dichroism spectra of the ODN/cDNA (a) and ODN/cRNA (b).
The duplexes contain 5′-d(GCGTTTTTTGCT)-3′ (black line, ODN**1**), 5′-d(GCGTT**B**TTTGCT)-3′ (green line, ODN**2**), 5′-d(GCGT**B**T**B**TTGCT)-3′ (light blue line, dashed, ODN**3**), 5′-d(GCGTT**BB**TTGCT)-3′ (blue line, ODN**4**), 5′-d(GCG**B**T**B**T**B**TGCT)-3′ (dark red line, dashed, ODN**5**), and 5′-d(GCGT**BBB**TTGCT)-3′ (red line, ODN**6**) in the ODN. The cDNA and cRNA are 5′-d(AGCAAAAAACGC)-3′ (cDNA**1**) and 5′-r(AGCAAAAAACGC)-3′ (cRNA**1**), respectively. Conditions: 2 mM sodium phosphate buffer (pH 7.2), 20 mM NaCl. The concentrations of ODNs and cDNA or cRNA were 2 μM for each strand. Measurements were performed at 10 °C. **B**: OBN.

5′-d(GCGTT**X**TTTGCT)-3′ (ODN)
3′- (CGCAA**Y**AAACGA)-5′ (ssDNA or ssRNA)

(a) ODN/ssDNA

X	T_m value (ΔT_m: T_m[mismatch] – T_m[match]) (°C)			
Y =	A	G	T	C
T	40	25 (-15)	24 (-16)	23 (-17)
B	40	30 (-10)	27 (-13)	23 (-17)

(b) ODN/ssRNA

X	T_m value (ΔT_m: T_m[mismatch] – T_m[match]) (°C)			
Y =	A	G	U	C
T	37	31 (-6)	21 (-16)	18 (-19)
B	41	36 (-5)	26 (-15)	25 (-16)

The measurement buffer conditions were the same as those listed in Table 1. X denotes T (= thymidine, ODN1) or **B** (= OBN, ODN**2**). Y indicates A, G, T (or U), and C. ΔT_m/mod. = the change in T_m value (ΔT_m) of each ODN containing mismatch nucleobases relative to the matched sequence (ODN**1** or ODN**2**).

In this experiment, ODN**2** was selected because of its pronounced duplex-forming ability toward ssDNA and ssRNA. ΔT_m values were re-defined as the gap between the match sequence and mismatched sequences in each ODN with DNA or RNA complement. Each base pair pattern of X and Y is abbreviated as X:Y. Each T_m value of the mismatched sequence in ODN**2**/ssDNA is 30 °C (**B**:G), 27 °C (**B**:T), and 23 °C (**B**:C). The values in ODN**1**/ssDNA were 25 °C (T:G), 24 °C (T:T), and 23 °C (T:C). In addition, ΔT_m values compared with matched sequences (**B**:A) were -10 °C (**B**:G), -13 °C (**B**:T), and -17 °C (**B**:C). These ΔT_m values compared with those of ODN1/ssDNA were decreased by 5 °C for guanine [T:G (-15 °C) vs. **B**:G (-10 °C)] and 3 °C against thymine [T:T (-16 °C) vs. **B**:T (-13 °C)]. The same values were evident concerning cytosine [T:C (-17 °C) vs. **B**:C (-17 °C)]. ODN**2** stabilized the formation of mismatch base pairs in comparison with ODN**1**, preferentially forming hydrogen bonds with adenine.

In the duplex of ODN**2**/ssRNA, the T_m values were 36 °C (**B**:G), 26 °C (**B**:U), and 25 °C (**B**:C). In addition, the ones in ODN**1**/ssRNA were 31 °C (T:G), 21 °C (T:U), and 18 °C (T:C). In addition, ΔT_m values were -5 °C (**B**:G), -15 °C (**B**:U), and -16 °C (**B**:C) compared with the matched sequence of ODN**2**/ssRNA (**B**:A). In comparison to ΔT_m values of ODN, mismatch discrimination of ODN**2**/ssRNA decreased by 1 °C against both guanine and uracil [(T:G (-6 °C) vs. **B**:G (-5 °C)] and [T:U (-16 °C) vs. **B**:U (-15 °C)] and 3 °C against cytosine [T:C (-19 °C) vs. **B**:C (-16 °C)]. Reviewing these ΔT_m values, it can be presumed that the stacking interaction due to OBN non-specifically stabilized all mismatch base pairs. In addition, the ΔT_m value against guanine (**B**:G) in ODN**2**/ssRNA was -5 °C. This ΔT_m value was narrower than that of other mismatch base pairs (**B**:U or **B**:C). This result may involve the formation of wobble base pairs[28] between thymine (uracil) and guanine in DNA/RNA duplexes (ΔT_m: -6 °C (T:G) in ODN**1**/ssRNA), which may also be applied to ODN**2**/ssRNA in the same manner, considering that OBN is a thymidine analog. Overall, mismatch discrimination of OBN decreased in comparison with thymine. However, the discrimination pattern of OBN was similar to that of natural thymine.

Circular dichroism (CD) spectra

The duplex structure of OBN-modified ODNs**2-6**/cDNA**1** or /cRNA**1** was evaluated by measuring the CD spectra (Fig. 3). In the duplex of OBN-modified ODNs**1-6** and cDNA**1**, canonical B-form structures were predominant in each duplex. With regard to single modification, both singly OBN- and bT-dR-

modified ODNs/cDNA often did not induce significant helical distortion. However, duplexes with consecutive OBN-modified ODN**4** and, especially, ODN**6**/cDNA**1** displayed characteristic negative and positive cotton bands at approximately 320 nm and 350 nm, respectively, in comparison with ODN**1**, **2**, **3** and **5**/cDNA**1**. One possibility is that ODN **4** and **6**/cDNA**1** can induce a structural change by strong stacking interaction. However, it is likely that this alteration did not deteriorate the duplex stability caused by OBN.

On the other hand, each of the double helices of ODN**1**-**6**/cRNA**1** described typical A-form helices with cRNA**1** without significant changes in the CD spectra. Each spectrum suggested that these duplex structures composed of ODNs and cRNA**1** were generally stabilized by modification of OBN. There was no significant distortion, even if three consecutive

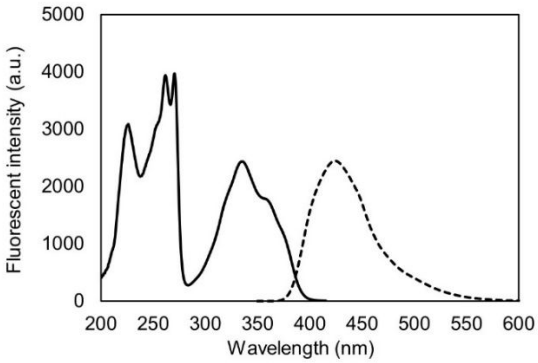

Fig. 4 Excitation and emission spectra of OBN nucleoside monomer (**6**). Conditions: 2 mM phosphate buffer (pH 7.2), 4 μM of **6**. Plain; 425 nm of emission wavelength, dashed; 335 nm of excitation wavelength.

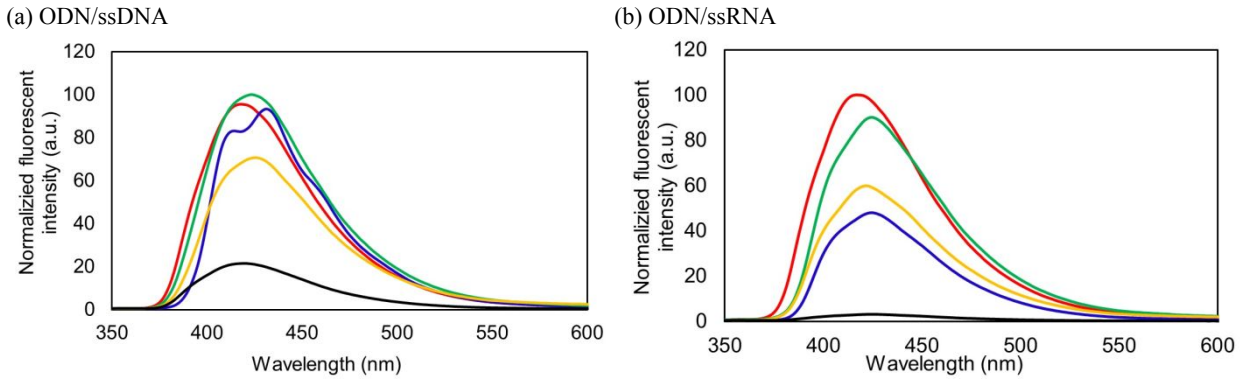

Fig. 5 Fluorescent spectra of OBN-modified ODN2 duplexes with ssDNA (a) and ssRNA (b).
Conditions: 2 mM sodium phosphate buffer (pH 7.2) containing 20 mM NaCl at 10 °C. The oligonucleotide concentration was 2 μM for each strand. Sequence: 5′-d(GCGTT**B**TTTGCT)-3′ (ODN**2**)/3′-d(CGCAAYAAACGA)-5′ (ssDNA) or /3′-r(CGCAAYAAACGA)-5′ (ssRNA) (Y: G <black>, A <blue>, T (or U) <green>, and C <yellow>). The spectrum of only ODN**2** is shown in red.

OBNs were incorporated in ODN**6**. This result was consistent with the MD simulation that the duplex structure was maintained by the three consecutive OBNs in ODN**6** toward cRNA**1** (Fig. 2)

Fluorescence derived from structure of OBN

The fluorescent properties derived from the OBN monomer or structure, and the fluorescence spectra of duplexes of OBN-modified ODN**2**/ssDNA and /ssRNA were investigated. The OBN nucleoside was excited at 335 nm. The maximum emission wavelength was observed at 425 nm in phosphate buffer (2 mM, pH 7.2, containing 20 mM NaCl; Fig. 4). Considering that bT-dR was excited at 321 nm and emitted at approximately 370 nm, incorporation of a benzene ring into OBN contributed to a longer emission wavelength than bT-dR (from 48 to 90 nm)[25]. A similar strategy has already been reported in which some nucleosides with artificial nucleobases can acquire longer maximum emission wavelength (39-67 nm) due to incorporation of benzene than those not containing a benzene structure (yyT and yyC) [29]. The findings suggest that extending the conjugation in the nucleobase could be a rational approach to induce a red shift of a nucleobase with a fluorescent spectrum. In addition, the OBN monomer displayed a quantum yield (φ) of 9.6% quantum yield. The φ was determined using quinine sulfate dihydrate as a reference. Given that the φ of the bT monomer was 5.1-5.9%, a slightly larger φ was observed in the OBN monomer[25]. The Stokes shift of the duplex containing the OBN-modified ODN was 90 nm (excited at 335 nm and emitted at 425 nm), which was almost the same as the tCo structure (excited at 360 nm and emitted at 450 nm)[23b], but was larger than the bT structure (excited at 329 nm and emitted at 375 nm)[25].

The fluorescence spectra of ODN**2**/ssDNA or /ssRNA containing match (A) and three mismatches (C, G, and T (U)) nucleobases were measured (Fig. 5). For the duplex of OBN-modified ODNs and ssDNA, the fluorescence intensity was in the order ODN**2**/ssDNA (T-mismatch, **B**:T) ≥ ODN**2** ≥ ODN**2**/ssDNA (A-match, **B**:A) > ODN**2**/ssDNA (C-mismatch, **B**:C) >> ODN**2**/ssDNA (G-mismatch, **B**:G). In the duplexes with ssRNA, the fluorescence intensity was observed in the order ODN**2** > ODN**2**/ssRNA (U-mismatch, **B**:U) >

ODN**2**/ssRNA (C-mismatch, **B**:C) > ODN**2**/ssRNA (A-match, **B**:A) >> ODN**2**/ssRNA (G-mismatch, **B**:G). It was shown that the fluorescent intensity of ODN**2** strongly weakened, particularly when the duplexes ODN**2**/ssDNA and /ssRNA (G-mismatch, **B**:G) were formed. This result was mainly explained that guanine nucleobase induces fluorescent quenching caused by the photoinduced electron transfer (PeT) system[30]. However, considering that T_m values of ODN**2**/ssDNA and /ssRNA (G-mismatch, **B**:G) were relatively higher than ODN**2**/ssDNA and /ssRNA containing other mismatches (**B**:T (or U) and **B**;C), this fluorescent quenching is caused by PeT of guanine, and base pairing of **B**:G to some extent, simultaneously[31]. With regard to ODN**2**/ssDNA and /ssRNA (A-match, **B**:A), two distinctive features were observed. First, in the duplex of ODN**2**/ssDNA (**B**:A), different peak patterns were observed in other spectra. Second, the quenching level of ODN**2**/ssRNA (**B**:A) was greater than that of ODN**2**/ssDNA (**B**:A). This result might be related to the slightly higher T_m value of ODN**2**/ssRNA (**B**:A) than ODN**2**/ssDNA (**B**:A). In addition, the pKa of OBN proton by fluorescent intensity level in each pH buffer condition was assessed[31], but the pKa of ODN**2** was not dependent on pH (Fig. S7).

Overall, because OBN exhibited maximum emission at 425 nm in ODN, which is red-shifted in comparison with bT, the observation of OBN could be used for imaging techniques.

Triplex-forming ability

Seven types of triplex-forming oligonucleotides (TFOs), which contain OBN in different positions, were designed based on TFO**1** to investigate the effect of the adjacent nucleobase of OBN. TFO**1** was designed to form a parallel DNA triple helix toward dsDNA (Table 3, Fig. S8). In addition, 7 mM sodium phosphate buffer (pH 7.0 or 6.0), 140 mM KCl, and 10 mM $MgCl_2$ were used in this measurement.

The T_m value of TFO**1**/dsDNA at pH 7.0 was 39 °C. The T_m value (ΔT_m value in comparison with TFO**1**/dsDNA) for TFO**2**, TFO**3**, and TFO**4**/dsDNA was 42 °C (+3 °C), 37 °C (-2 °C), and 39 °C (±0 °C), respectively. Based on these results, 2′-deoxy-5-methylcytidine (abbreviated to C in ODN) of both the 5′-side and 3′-sides, especially the latter, against OBN did not involve in enhancing the triplex-forming ability. It is conceivable that

Table 3 T_m values (°C) of triplexes formed between TFO and hairpin-double strand (ds) DNA

Sequence, 5′→3′	T_m (ΔT_m /mod.) (°C)	
	pH 7.0	pH 6.0
TFO**1**: TTTTTCTTTCTCTCT	39	61
TFO**2**: TTTTTC**B**TCTCTCT	42 (+3)	64 (+3)
TFO**3**: TTTT**B**CTTTCTCTCT	37 (-2)	58 (-3)
TFO**4**: TTTTTC**B**TTCTCTCT	39 (±0)	61 (±0)
TFO**5**: TTTT**B**C**B**TTCTCTCT	37 (-1.0)	58 (-1.5)
TFO**6**: TTTT**B**CTT**B**CTCTCT	32 (-3.5)	54 (-3.5)
TFO**7**: TTTTTC**BB**TCTCTCT	45 (+3.0)	68 (+3.5)
TFO**8**: TTTTTC**BBB**CTCTCT	43 (+1.3)	69 (+2.7)

Conditions: 7 mM sodium phosphate buffer (pH 7.0 or 6.0) containing 140 mM KCl, 10 mM $MgCl_2$, and 1.5 μM of each ODN. The sequence of target hairpin dsDNA was 5′-d(GGC*AAAAAGAAAGAGAGA*CGC)-Spacer 18 (HEG)-(GCG*TCTCTCTTTCTTTTT*CGC)-3′. TFO forms a triplex structure in the italicized sequence in dsDNA. C: 2′-deoxy-5-mehtylcytidine; **B**: OBN; HEG: hexaethylene glycol.

protonated cytosine in TFO can induce repulsion with OBN, which decreases the T_m values[33]. On the other hand, thymidine of both the 5′- and 3′-sides against OBN may improve the triplex-forming ability.

In TFOs modified by multiple OBN, the T_m (ΔT_m/mod.) value of TFO**5**/dsDNA was 37 °C (-1.0 °C). The finding suggested that the C of the 3′-side of one OBN decreases the T_m values. TFO**6**/dsDNA, which contains two Cs at the 3′-position of both OBNs, decreased the T_m (ΔT_m/mod.) values [32 °C (-3.5 °C)]. TFO7/dsDNA, in which two OBN were incorporated consecutively, displayed the highest T_m (ΔT_m/mod.) value of 45 °C (+3.0 °C) in all TFO sequences. The high T_m value was attributed to the presence of thymidine at the 3′-side of OBN. The T_m (ΔT_m/mod.) value of TFO**8**/dsDNA containing three consecutive OBN was 43 °C (+1.3 °C). This finding suggested that the incorporation of C at the 3′-position of one OBN decreased the T_m value in comparison with TFO**7**/dsDNA.

Considering these results, OBN-modified ODN could function as a TFO to improve the triplex-forming ability when the sequence was designed such that: (1) C was not positioned at the 3′-side of OBN and (2) the OBNs were consecutively modified. With respect to the triplex-forming ability, consecutively modified TFO**7** and **8**/dsDNA displayed higher T_m values than TFO**1**/dsDNA. In addition, the MD calculation result could support possibility of (2) and increased T_m values, indicating that consecutive OBNs continue to stack with flanking nucleobases (Fig. S9). Based on the fact that T_m value was decreased in DNA/ds(tT-PNA)[24a], consecutive OBN in ODN would be more suitable for dsDNA, rather than dsPNA, to obtain high triplex-forming ability.

Additionally, the hysteresis between melting and annealing curves in some sequences (TFO**1**, TFO**2**, TFO**7**) were investigated (Fig. S10). As a result, the hysteresis was observed only in TFO**7**/dsDNA with the ramp rate of 0.5 °C/min, but not observed with the one of 0.2 °C/min.

Enzymatic stability

The enzymatic resistance of OBN-modified ODN (ODN(T_9**B**)) against 3′-exonuclease (*Crotalus admanteus* venom phosphodiesterase) was investigated (Fig. 6). The 10-mer ODN containing OBN at the 3′-terminal position, 10-mer ODN composed of only natural thymidine (ODN**15**), and thymidine 10-mer ODNs including PS (phosphorothioate) modification as the 3′-terminal phosphodiester linkage (ODN**16**, (*S*)-optical isomer and ODN**17**, (*R*)-optical isomer) were simultaneously evaluated. These four ODNs were incubated with 3′-exonuclease for 40 min. The percentage of remaining intact ODNs with time was quantified by HPLC. More than 95% of the 3′-terminal OBN-modified 10-mer ODN**18** remained after 40 min, while no ODN**15** composed of only natural thymidine remained. The residual percentages of ODN**16** and ODN**17** at

40 min were 77% and 71%, respectively, indicating that ODN containing OBN obtained higher enzymatic stability than ODN, including PS modification.

Enhanced enzymatic resistance was obtained due to steric hindrance of nucleobase in OBN, because phenoxazine-and G-clamp-modified ODNs also indicated good enzymatic stability[34]. Therefore, it is expected that modification of the nucleobase accompanying steric hindrance can be a reasonable strategy for both high binding affinity and enzymatic stability. Furthermore, given that the *C*-nucleoside-like pseudouridine enhances the stability against nuclease[35], it would be assumed that OBN also improved enzymatic stability against CAVP by the effect of the *C*-nucleoside structure.

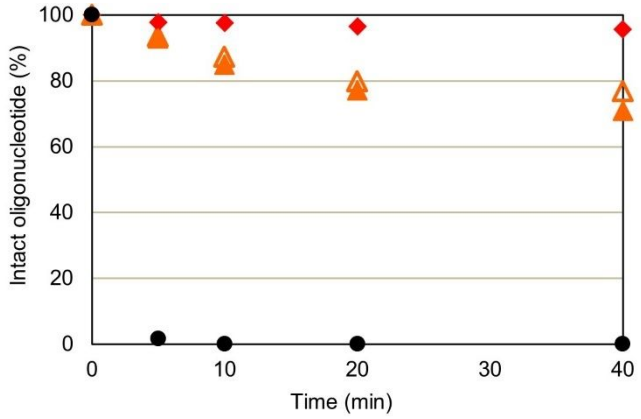

Fig. 6 Enzymatic stability of 3′-exonuclease (*Crotalus Admanteus* Venom Phosphodiesterase; CAVP).
Conditions: 0.4 μg/mL CAVP, 10 mM $MgCl_2$, 50 mM Tris-HCl (pH 8.0), and 4 μM of each oligonucleotide, incubated at 37 °C. Sequence: 5′-d(TTTTTTTTTT)-3′ (ODN**15**, black circle), 5′-d(TTTTTTTTTT^T)-3′; ^ denotes a phosphorothioate linkage applied only for PS_S_p (ODN**16**, open orange triangle) and PS_R_p (ODN**17**, closed orange triangle), and 5′-d(TTTTTTTTT**B**)-3′ (ODN**18**, red diamond). **B**: OBN.

Conclusions

In this paper, we report a tricyclic thymidine analog, the OBN monomer, and consecutively incorporated OBN into ODNs to obtain high duplex- and triplex-forming abilities compared with ODNs natural thymidine. OBN-modified ODNs showed higher enzymatic resistance than ODNs containing phosphorothioate (PS) modification, presumably due to steric hindrance caused by the tricyclic structure of the nucleobase. In addition, OBN-modified ODNs exhibited a new fluorescent wavelength. The collective results indicate that OBN-modified ODNs bearing consecutive modifications may be useful for application as DNA probes, for example, due to their fluorescent properties.

Experimental

General

Dehydrated acetone, acetonitrile, ethanol, dichloromethane, *N*,*N*-dimethylformamide (DMF), methanol, pyridine, and tetrahydrofuran (THF) were used as purchased. *N*,*N*-diisopropylethylamine (DIPEA) and *n*-tributylamine were used for the reaction after being distilled from the mixture with calcium hydride. ^1H, ^{13}C, and ^{31}P nuclear magnetic resonance (NMR) spectra were recorded on JEOL JNM-ECS300, JNM-ECS400, and JNM-ECA500 spectrometers. Chemical shifts were reported as δ values in parts per million (ppm) relative to internal tetramethylsilane (0.00 ppm), residual CHD_2OD (3.31 ppm), CHD_2CN (1.94 ppm), and $CHD_2S(=O)D_3$ (2.50 ppm) for ^1H NMR, chloroform-d_1 (77.2 ppm), methanol-d_4 (49.0 ppm), acetonitrile-d_3 (1.32 ppm), and DMSO-d_6 (39.5 ppm) for ^{13}C NMR, and 5% H_3PO_4 (0.00pm) for ^{31}P-NMR. The nS-8 oligonucleotide automated DNA synthesizer (Gene Design Inc.) was used. UV absorbance and UV melting experiments were performed using UV-1650PC or UV-1800 instruments (SHIMADZU). Infrared spectra were recorded on a JASCO FT/IR-4200 spectrometer. Fluorescence spectra were measured using a JASCO FP-8500 instrument. CD spectra were measured using a JASCO J-720W instrument. Optical rotations were recorded using a JASCO DIP-370 instrument. MALDI-TOF mass of all new compounds was measured using a JEOL SpiralTOF JMS-S3000 instrument. MALDI-TOF mass spectra of all ODNs were recorded on a Bruker Daltonics Autoflex II TOF/TOF mass spectrometer. For column chromatography, Silysia PSQ-100B, PSQ-60B, or FL-100D silica gels (Fuji) were utilized. For HPLC, CBM-20A, DGU-20A3, LC-20AT, CTO-20A, SPD-20A, and FRC-10A instruments (SHIMADZU) were utilized. All complementary ssDNA or ssRNA used for the UV melting experiments were purchased from GeneDesign, Inc.

1,2-Dihydro-2-oxobenzo[*b*][1,8]naphthyridine-3-calboxylic acid (2)

A solution of ethyl-1,2-dihydro-2-oxobenzo[*b*][1,8]naphthyridine-3-carboxylate (**1**) (2.69 g, 10.0 mmol) in THF/H_2O (15 ml each) was prepared. Lithium hydroxide monohydrate (2.02 g, 48.1 mmol) was added, and the resultant mixture was stirred for 2 h at 70 °C. The mixture was cooled to room temperature. After the addition of saturated aqueous NH_4Cl solution following aqueous HCl (40 mL, 1.0 M) solution to neutralize the pH, the yellow precipitate was filtered under reduced pressure. The precipitate was washed well with H_2O and THF, and then dried in vacuo to obtain compound **2** as a yellow solid (2.05 g, 8.53 mmol, 85%); mp: >300 °C. $[\alpha]_D^{24}$ +1.78 (c 0.1, DMSO); IR ν_{max} (KBr): 3161, 1662, 1624, 1564, 1506, 1479, 1400, 1313, 1279, 1246, 1223, 1184, 967 cm^{-1}; ^1H NMR (400 MHz, DMSO-d_6): δ 7.24 (1H, t, J = 8.0 Hz), 7.57 (1H, t, J = 6.0 Hz), 7.74 (1H, d, J = 8.0 Hz), 7.84 (1H, d, J = 8.0 Hz), 8.29 (1H, s), 8.42 (1H, s); ^{13}C NMR (125.8 MHz, DMSO-d_6): δ 115.5, 125.1, 127.1, 129.0, 132.1, 139.0, 142.0, 148.1, 149.0, 165.1, 165.3; HRMS (MALDI) Calcd. for $C_{13}H_9N_2O_3$ $[M+H]^+$: 241.0608, Found: 241.0608.

3-Bromo-1,2-dihydro-2-oxobenzo[*b*][1, 8]naphthyridine (3)

A solution containing Br_2 (0.035 mL, 6.8 mmol) in DMF/pyridine (5 mL/2.5mL) was prepared. Compound **2** was added at 0 °C and the reaction mixture was stirred at 105 °C for 1 h under an argon (Ar) atmosphere. The resulting mixture was cooled to room temperature and then poured into crushed ice.

The desired brown precipitate, representing **3**, was filtered under reduced pressure, and washed thoroughly with methanol (MeOH) following H_2O washing. The filtrate was concentrated, and which was washed as above three times to afford compound **3** as a brown solid (136 mg, 0.494 mmol, 81 %); $[\alpha]_D^{24}$ -16.6 (c 1.0, DMSO); IR ν_{max} (KBr): 3617, 3518, 3114, 3061, 1964, 1672, 1614, 1588, 1504, 1471, 1452, 1389, 1304, 1273, 1237, 1177, 1011 cm^{-1}; ^1H NMR (500 MHz, DMSO-d_6): δ 7.55 (1H, td, J = 7.5, 1.3 Hz), 7.83 (1H, td, J = 7.5, 1.5 Hz), 7.90 (1H, bd, J = 8.0 Hz), 8.06 (1H, bd, J = 8.0 Hz), 8.66 (1H, s), 8.73 (1H, s); ^{13}C NMR (100.5 MHz, DMSO-d_6): δ 115.7, 118.7, 124.7, 125.2, 127.1, 128.9, 131.8, 136.6, 140.3, 147.4, 148.3, 158.9; HRMS (MALDI) Calcd. for $C_{12}H_8N_2OBr$ $[M+H]^+$: 274.9819, Found: 274.9815.

1′-β-[3-(1,2-Dihydro-2-oxobenzo[*b*][1,8]naphthyridine)]-2′-deoxy-D-ribofuranose (6)

$Pd_2(dba)_3$ (190 mg, 0.208 mmol) and P(*o*-tol)$_3$ (196 mg, 0.645 mmol) were suspended in 1,4-dioxane (20 mL) after freeze-pump-thaw cycling) and stirred for 30 min at room temperature under an Ar atmosphere. Compound **3** (403 mg, 1.46 mmol) and 1,4-anhydro-3-*O*-(tert-butyldiphenylsilyl)-2-deoxy-D-erythro-pent-1-enitol[27] (500 mg, 1.41 mmol) were added to the solution and distilled in *n*-Bu_3N (0.70 mL, 2.9 mmol) with stirring at 75 °C for 18 h under an Ar atmosphere. After the reaction mixture was filtered with Celite, the filtrate was concentrated under reduced pressure and purified by silica gel column chromatography ($CHCl_3$: MeOH = 95:5) to obtain a precipitate containing **4** (855 mg). A solution of AcOH/THF (1.5 mL/10 mL) containing compound **4** (855 mg) received TBAF (1 M in THF, 1.5 mL, 1.5 mmol) at 0 °C. The resulting solution was stirred at 0 °C for 20 min under an Ar atmosphere. After the addition of saturated aqueous NH_4Cl solution at 0 °C, the resulting mixture was extracted with ethyl acetate (AcOEt). The organic extracts were dried over Na_2SO_4, and the residue was concentrated under reduced pressure and purified again by silica gel column chromatography (*n*-hexane : AcOEt = 1:3) to produce a mixture of compound **5** (145 mg). A AcOH/MeCN (2 mL/10 mL) solution containing compound **5** (145 mg) received $NaBH(OAc)_3$ (305 mg, 1.44 mmol) at -20 °C. The reaction mixture was stirred for 20 min at -20 °C under an Ar atmosphere. After the addition of MeOH at -20 °C, the resulting mixture was concentrated with toluene to remove all solvents under reduced pressure. The residue was purified by silica gel column chromatography (AcOEt : MeOH = 95:5) to afford pure compound **6** as a yellow solid (103 mg, 0.328 mmol, 23% over three steps); mp: 122-126 °C. $[\alpha]_D^{24}$ +62.5 (c 0.2, MeOH); IR ν_{max} (KBr): 3354, 3056, 2925, 2338, 2073, 1653, 1618, 1584, 1569, 1505, 1463, 1398, 1325, 1245, 1177, 1053 cm^{-1}; ^1H NMR (300 MHz, MeOH-d_4): δ 1.88-1.98 (1H, m), 2.46-2.54 (1H, m), 3.69-3.79 (2H, m), 3.99-4.03 (1H, m), 4.32-4.36 (1H, m), 5.25-5.30 (1H, m), 7.49-7.55 (1H,m), 7.75-7.81 (1H, m), 7.95 (1H, d, J = 9.0 Hz), 7.99 (1H, d, J = 6.0 Hz), 8.22 (1H, bs), 8.62 (1H,bs); ^{13}C NMR (125.8 MHz, MeOH-d_4): δ 42.7, 64.0, 74.2, 77.0, 88.8, 117.1, 126.2, 126.9, 128.5, 129.6, 132.5, 134.8, 136.9, 138.1, 149.1, 149.4, 164.8; HRMS (MALDI) Calcd. for $C_{17}H_{17}N_2O_4$ $[M+H]^+$: 313.1184, Found: 313.1183.

1′-β-[3-(1,2-Dihydro-2-oxobenzo[*b*][1,8]naphthyridine)]-5′-*O*-(4,4′-dimethoxytrityl)-2′-deoxy-D-ribofuranose (7)

A solution of compound **6** (144 mg, 0.462 mmol) in pyridine (5 mL) was prepared. 4,4'-Dimethoxytrityl chloride (DMTrCl; 204 mg, 0.601 mmol) was added at 0 °C. The reaction mixture was stirred at room temperature for 4 h under an Ar atmosphere. After the addition of saturated aqueous $NaHCO_3$ solution at 0 °C, the resulting residue was extracted with AcOEt. The organic extracts were washed with H_2O, dried over Na_2SO_4, and concentrated under reduced pressure. The residue was purified by silica gel column chromatography (*n*-hexane : AcOEt = 1:3) to afford compound **7** (248 mg, 0.402 mmol, 87%) as a yellow amorphous solid; mp: 122-126 °C. $[\alpha]_D^{24}$ -20.5 (c 1.0, $CHCl_3$); IR ν_{max} (KBr): 3412, 3121, 3060, 3007, 2930, 2836, 2046, 1903, 1660, 1619, 1572, 1508, 1463, 1443, 1395, 1301, 1249, 1176, 1152, 1085, 1038 cm^{-1}; ^1H NMR (400 MHz, $CDCl_3$): δ 1.85 (1H, d, J = 4.2 Hz), 2.03-2.10 (1H, m), 2.60-2.66 (2H, m), 3.38-3.45 (2H, m), 3.75 (3H, s), 3.75 (3H, s), 4.11-4.15 (1H, m), 4.45-4.49 (1H, m), 5.39 (1H, t, J = 7.5 Hz), 6.83 (4H, d, J = 8.8 Hz), 7.21-7.24 (1H, m), 7.27-7.31 (2H, m), 7.38 (4H, d, J = 8.9Hz), 7.47-7.52 (3H, m), 7.74-7.81 (2H, m), 8.00 (2H, t, J = 4.1 Hz), 8.12 (1H, d, J = 1.4 Hz), 9.36 (1H, bs); ^{13}C NMR (125.8 MHz, $CDCl_3$): δ 41.8, 55.0, 55.3, 64.0, 73.6, 75.2, 77.4, 85.6, 86.4, 113.3, 115.9, 125.2, 125.5, 127.0, 127.8, 128.0, 128.4, 128.4, 130.3, 131.4, 132.9, 136.1, 136.2, 136.8, 136.8, 145.0, 147.6, 148.2, 158.6, 163.1; HRMS (MALDI) Calcd. for $C_{38}H_{34}N_2O_6Na$ $[M+Na]^+$: 637.2309, Found: 637.2305.

1′-β-[3-(1,2-Dihydro-2-oxobenzo[*b*][1,8]naphthyridine)]-5′-*O*-(4,4′-dimethoxytrityl)-2′-deoxy-D-ribofuranose-3′-(2-cyanoethyl tetraisopropylphosphoramidite) (8)

A solution of compound of **7** (171 mg, 0.277 mmol) in CH_2Cl_2 (8 mL) was prepared. DIPEA (0.12 mL, 0.69 mmol) and 2-cyanoethyl diisopropyl chlorophosphoramidite (0.080 mL, 0.36 mmol) were added at 0 °C. The reaction mixture was stirred at room temperature for 3 h under an Ar atmosphere. After the addition of H_2O at 0 °C, the resulting residue was extracted with AcOEt. The organic extracts were washed with H_2O, dried over Na_2SO_4, and concentrated under reduced pressure. The residue was purified by silica gel column chromatography (*n*-hexane : AcOEt = from 1:1 to 1:2) to afford compound **8** (220 mg, 0.270 mmol, 98%) as a yellow amorphous solid; ^1H NMR (300 MHz, $CDCl_3$): δ 0.83-1.39 (12H, m), 2.00-2.12 (1H, m), 2.44 (6/10 2H, t, J = 7.5 Hz), 2.64 (4/10 2H, t, J = 6.0 Hz), 2.68-2.81 (1H, m), 3.30-3.38 (1H, m), 3.43-3.64 (4H, m), 3.74 (3H, s), 3.75 (3H, s), 3.77-3.91 (1H, m), 4.20-4.26 (1H, m), 4.50-4.65 (1H, m), 5.40 (1H, t, J = 7.5 Hz), 6.80-6.86 (4H, m), 7.19-7.26 (1H, m), 7.27-7.33 (2H, m), 7.36-7.43 (4H, m), 7.45-7.54 (3H, m), 7.74-7.80 (2H, m), 7.84 (6/10H, s), 7.83(4/10H, s), 8.04-8.05 (6/10H, m), 8.07-8.07 (4/10H, m), 8.17 (4/10H, d, J = 1.3 Hz), 8.23 (6/10H, d, J =1.3 Hz), 9.77 (6/10H, bs), 9.85 (4/10H, bs); ^{31}P NMR (121.7 MHz,

$CDCl_3$): δ 147.8, 148.6; HRMS (MALDI) Calcd. for $C_{47}H_{51}N_4O_7NaP$ $[M+Na]^+$: 837.3388, Found: 837.3405.

Assessment of molecular absorptivity of OBN nucleoside

The UV spectrum for molecular absorptivity (ε) was measured using a UV-1800 spectrometer (SHIMADZU). The ε was calculated using the Lambert-Beer law. OBN nucleoside was dissolved in H_2O containing 0.1% (v/v) DMSO (25 μM final concentration).

Synthesis and identification of OBN-incorporated oligonucleotides

OBN-incorporated oligonucleotides were synthesized at 0.2 μmol scale. 5-[3,5-Bis(trifluoromethyl)phenyl]-1*H*-tetrazole was used as the activator for all coupling steps. The coupling time of standard phosphoramidite increased from 25 s to 2.5 min. While both the OBN phosphoramidite unit **8** and other unmodified phosporamidites were prepared in (MeCN 0.10 M), the coupling times of the latter were 25 s (as a standard protocol). The ODNs were synthesized in the DMTr-on mode. Solid (CPG)-supported ODNs were cleaved and the protected groups of each nucleobase and phosphordiester linkages were removed with a mixed solution of 40% aqueous methylamine and 28% aqueous ammonia solution (the ratio was 1:1 in v/v) for 10 min at 65 °C. The crude ODNs bearing a DMTr group were removed and purified with a Sep-Pak® Plus C18 Cartridge and Sep-Pak® Plus C18 Environmental Cartridge (Waters), washed with 10% aqueous MeCN solution, detritylated with 0.5% aqueous trifluoroacetic acid solution, and eluted with 35% aqueous MeOH solution. Reverse-phase HPLC was performed using a Waters XBridge™ OST C18 2.5 μm (10×50 mm) and 0.1 M triethylammonium acetate (TEAA) buffer (pH 7.0) as buffer A and 100% MeCN as buffer B. The compositive confirmation of purified ODNs was performed by reverse-phase HPLC on a Waters XBridge™ OST C18 2.5 μm (4.6×50 mm) and by MALDI-TOF mass spectrometry.

Thermal denaturation experiments (duplex-forming ability)

The UV melting profiles were recorded in 2 mM sodium phosphate buffer (pH 7.2) containing 20 mM NaCl to obtain a final concentration of each ODN at 2 μM. The sample mixtures were annealed by heating at 100 °C, followed by slow cooling to room temperature. The melting profiles were recorded at 260 nm from 5 to 90 °C at a scan rate of 0.5 °C/min. T_m values were calculated as the temperature of the half-dissociation of the duplex in the melting curve.

Snapshots of MD

In Fig. 2 and S9, the MDs were recorded using MacroModel software (Schrödinger, LLC) using OPLS3 force field (in H_2O at 300 K, with 1.5 fs time steps, an equilibration time of 1.0 ps and a 30 ns simulation time. Before the MD simulation was performed, the initial duplex (Fig. 2) and triplex (Fig. S9) were optimized using OPLS3 in H_2O.

CD spectra measurements

The spectra were recorded in a quartz cuvette with an optical path length of 1 cm at 10 °C. The samples were prepared in the same manner as described for the UV melting experiments. The molar ellipticity was calculated from the equation $[\theta] = \theta/cl$, where θ indicates the relative intensity, "c" describes the sample concentration, and "l" is the cell path length in cm.

Thermal denaturation experiments (triplex-forming ability)

The UV melting profiles were recorded in 7 mM sodium phosphate buffer (pH 6.0 or 7.0) containing aqueous 140 mM KCl and 10 mM $MgCl_2$ to give final concentration of each ODN for 1.5 μM. The sample mixtures were annealed by heating at 100 °C, followed by slow cooling to room temperature. The melting profile was recorded at 260 nm from 5 to 90 °C at a scan rate of 0.5 °C/min. The T_m values were calculated by the differential method as the temperature of the half-dissociation of the triplex based on the melting curve.

Measurements of fluorescence properties

The fluorescence properties of OBN nucleoside (**6**) were recorded in 2 mM sodium phosphate buffer (pH 7.2) containing 4 μM of **6** (Fig. 4). The fluorescence properties of ODN**2**/ssDNA and /ssRNA were measured in 2 mM sodium phosphate buffer (pH 7.2) containing 20 mM NaCl to give a final concentration of each oligonucleotide at 2 μM (Fig. 5, S7). The fluorescence spectra were recorded using a JASCO FP-8500 fluorescence spectrophotometer. All spectra were recorded at 10 °C using a quartz cuvette with an optical path length of 1 cm.

Fluorescence quantum yield

The quantum yield (φ) of the OBN nucleoside was calculated using quinine sulfate dihydrate (φ = 0.55) in sulfuric acid (0.10 M). The emission spectrum area was integrated using the instrumentation software, and the quantum yield (φ) was calculated using the following equation:

$$\varphi_{(S)}/\varphi_{(R)} = [A_{(S)}/A_{(R)}] \times [Abs_{(S)}/Abs_{(R)}] \times [n_{(S)}^2/n_{(R)}^2]$$

where $\varphi_{(S)}$ and $\varphi_{(R)}$ indicate the quantum yields (φ) of the sample and reference, respectively, and the terms $A_{(S)}$ and $A_{(R)}$ refer to the areas under the fluorescence spectra of the sample and reference, respectively. $Abs_{(S)}$ and $Abs_{(R)}$ indicate the optical densities of the sample and reference solutions at the excitation wavelength, respectively. $n_{(S)}^2/n_{(R)}^2$ indicate the values of the refractive indices of the solvents used for the sample ($n_{(S)} = 1.332$) and reference ($n_{(R)} = 1.334$), respectively. Measurements were performed in 2 mM sodium phosphate buffer (pH 7.2), 20 mM NaCl, and 4 μM nucleoside (**6**) at 25 °C and excited at 335 nm.

Assessment of enzymatic stability of OBN-incorporated oligonucleotides

After sample solutions (250 μL) containing ODN**15**, **16**, **17**, and **18** (final concentration of each ODN was 4 μM) were prepared with $MgCl_2$ aq. (final concentration was 10 μM), Tris-HCl buffer (final concentration was 50 μM), and 3′-exonuclease

(CAVP; 0.40 μg/mL), and these solutions were incubated at 37 °C. Since the reaction was started, 50 μL of each solution was picked up and 3′-exonuclease was inactivated to heat at 90 °C for 5 min at each time point (5, 10, 20, and 40 min). The remaining amounts of each intact (full-length) oligonucleotide were analyzed and quantified using reverse-phase HPLC.

Conflicts of interest

The authors declare no conflict of interest.

Acknowledgements

This study was supported by the Core Research for Evolutional Science and Technology (CREST) program of the Japan Science and Technology Agency (JST), JSPS KAKENHI grant no. 15K08024 (O.N.) and 19J10113 (Y.K.), and the Basic Science and Platform Technology Program for Innovative Biological Medicine from the Japan Agency for Medical Research and Development (AMED) under Grant No. JP18am0301004. This research was also partially supported by the Platform Project for Supporting Drug Discovery and Life Science Research from AMED.

Notes and references

1 T. Yamamoto, M. Harada-Shiba, M. Nakatani, S. Wada, H. Yasuhara, K. Narukawa, K. Sasaki, M. Shibata, H. Torigoe, T. Yamaoka, T. Imanishi and S. Obika, *Mol. Ther. Nucleic Acids* **2012**, *1,* e22; V. Rottiers, S. Obad, A. Petri, R. McGarrah, M. W. Lindholm, J. C. Black, S. Sinha, R. J. Goody, M. S. Lawrence, A. S. deLemos, H. F. Hansen, S. Whittaker, S. Henry, R. Brookes, S. H. Najafi-Shoushtari, R. T. Chung, J. R. Whetstine, R. E. Gerszten, S. Kauppinen and A. M. Näär, *Sci. Transl. Med.* **2013**, *5,* 212ra162.

2 Y. Taniguchi, Y. Magata, T. Osuki, R. Notomi, L. Wang, H. Okamura and S. Sasaki, *Org. Biomol Chem.*, 2020, **18**, 2845-2851.

3 J. K. Nair, J. L. S. Willoughby, A. Chan, K. Charisse, Md. R. Alam, Q. Wang, M. Hoekstra, P. Kandasamy, A. V. Kel'in, S. Milstein, N. Taneja, J. O'Shea, S. Shaikh, L. Zhang, R. J. van der Sluis, M. E. Jung, A. Akinc, R. Hutabarat, S. Kuchimanchi, K. Fitzgerald, T. Zimmermann, T. J. C. van Berkel, M. A. Maier, K. G. Rajeev and M. Manoharan, *J. Am. Chem. Soc.*, 2014, **136**, 16958-16961; R. Parmar, J. L. S. Willoughby, J. Liu, D. J. Foster, B. Brigham, C. S.Theile, K. Charisse, A. Akinc, E. Guidry, Y. Pei, W. Strapps, M. Cancilla, M. G. Stanton, K. G. Rajeev, L. Sepp-Lorenzino, M. Manoharan, R. Meyers, M. A. Maier and V. Jadhav, *ChemBioChem*, 2016, **17**, 985-989.

4 R. Gambari, M. Borgatti, V. Bezzerri, E. Nicolis, I. Lampronti, M. C. Dechecchi, I. Mancini, A. Tamanini and G. Cabrini, *Biochem. Pharmacol.*, 2010, **80**, 1887-1894.

5 A. S. Jørgensen, L. H. Hansen, B. Vester, J. Wengel, *Bioorg. Med. Chem. Lett.*, 2014, **24**, 2273-2277; F. J. Hernandez, N. Kalra, J. Wengel, B. Vesters, *Bioorg. Med. Chem. Lett.*, 2009, **19**, 6585-6587; C. Förster, M. Zydek, M. Rothkegel, Z. Wu, C. Gallin, R. Geßner, F. Lisdat and J. P. Fürste, *Biochem. Biophys. Res. Commun.*, 2012, **419**, 60-65; G. Ying, X. Lu, J. Mei, Y. Zhang, J. Chen, X. Wang, Z. -M. Ou and Y. Yi, *Bioorg. Med. Chem.,*2019, **27**, 3201-3207.

6 J. Vollmer, J. S. Jepsen, E. Uhlmann, C. Schetter, M. Jurk, T. Wader, M. Wüllner, and Arthur M. Krieg, *Oligonucleotides*, 2004, **14**, 23-31; M. J. Lange, D. H. Burke and John C. Chaput, *Nucleic Acid Ther.*, 2019, **29**, 51-59.

7 M. Castoldi, V. Benes, M. W. Hentze and M. U. Muckenthaler, *Methods*, 2007, **43**, 146-152; A. Valoczi, C. Hornyik, N. Varga, J. Burgyan, S. Kauppinen and Z. Havelda, *Nucleic Acids Res.*, 2004, **32**, e175; W. P. Kloosterman, E. Wienholds, E. de Bruijn, S. Kauppinen and R. H. Plasterk, *Nat. Methods*, 2006, **3**, 27-29.

8 A. Hendel, R. O. Bak, J. T. Clark, A. B. Kennedy, D. E. Ryan, S. Roy, I. Steinfeld, B. D. Lunstad, R. J. Kaiser, A. B. Wilkens, R. Bacchetta, A. Tsalenko, D. Dellinger, L. Bruhn and M. H. Porteus, *Nat. Biotechnol.*, 2015, **33**, 985-989.

9 W. B. Wan and P. P. Seth, *J. Med. Chem.*, 2016, **59**, 9645-9667.

10 B. Cuenoud, F. Casset, D. Hüsken, F. Natt, R. M. Wolf, K.-H. Altmann, P. Martin, H. E. Moser, *Angew. Chem. Int. Ed.*, 1998, **37**, 1228-1291; M. J. J. Blommers, F. Natt, W. Jahnke, B. Cuenoud, *Biochemistry*, 1998, **37**, 17714-17725.

11 S. Obika, D. Nanbu, Y. Hari, K. Morio, Y. In, T. Ishida, T. Imanishi, *Tetrahedron Lett*., 1997, **38***,* 8735-8738; S. K. Singh, P. Nielsen, A. A. Koshkin, J. Wengel, *Chem. Commun*., 1998, **4**, 455-456; T. Imanishi, S. Obika, *Chem. Commun*., 2002, **16**, 1653-1659; S. Obika, D. Nanbu, Y. Hari, J. Andoh, K. Morio, T. Doi, T. Imanishi, *Tetrahedron Lett.,* 1998, **39**, 5401-5404; A. A. Koshkin, S. K. Singh, P. Nielsen, V. K. Rajwanshi, R. Kumar, M. Meldgaard, C. E. Olsen, J. Wengel, *Tetrahendon.,* 1998, **54**, 3607-3630.

12 S. Obika, Y. Hari, T. Sugimoto, M. Sekiguchi and T. Imanishi, *Tetrahedron Lett.*, 2000, **41**, 8923-8927; B. -W. Sun, B. R. Babu, M. D. Sørensen, K. Zakrzewska, J. Wengel and J. -S. Sun, *Biochemistry*, 2004, **43**, 4160-4169.

13 M. Winnacker and E. T. Kool, *Angew. Chem. Int. Ed.,* 2013, **52**, 12498-12508; J. Gao, H. Liu and E. T. Kool, *Angew. Chem. Int. Ed.,* 2005, **44**, 3118-3122.

14 H. Lu, K. He and E. T. Kool, *Angew. Chem. Int. Ed.,* 2004, **43**, 5834-5836; A. H. F. Lee and E. T. Kool, *J. Org. Chem.,* 2005, **70**, 132-140; A. H. F. Lee and E. T. Kool, *J. Am. Chem. Soc.,* 2005, **127**, 3332-3338; H. Lu, S. R. Lynch, A. H. F. Lee and E. T. Kool, *ChemBioChem*, 2009, **10**, 2530-2538.

15 C. A. Buhr, M. D. Matteucci, B. C. Froehler, *Tetrahedron Lett*. 1999, **40**, 8969-8970; A. Dierckx, F.-A. Miannay, N. B. Gaied, S. Preus, M. Björck, T. Brown, L. M. Wilhelmsson, *Chem. Eur. J.* 2012, **18**, 5987-5997; M. Bood, A. F. Fuchtbauer, M. S. Wranne, J. J. Ro, S. Sarangamath, A. H. El-Sagheer, D. L. M. Rupert, R. S. Fisher, S. W. Magennis, A. C. Jones, F. Höök, T. Brown, B. H. Kim, A. Dahlén, L. M. Wilhelmsson, M. Grøtli, *Chem. Sci.* 2018, **9**, 3494-3502.

16 D. A. Berry, K. Y. Jung, D. S. Wise, A. D. Sercel, W. H. Pearson, H. Mackie, J. B. Randolph, R. L. Somers, *Tetrahedron Lett.*, 2004, **45**, 2457-2461; F. Wojciechowski, R. H. E. Hudson, *J. Am. Chem. Soc.* 2008, **130**, 12574-12575.

17 S. Hirashima, J. H. Han, H. Tsuno, Y. Tanigaki, S. Park, H. Sugiyama, *Chem. Eur. J.*, 2019, **25**, 9913-9919; J. H. Han, S. Hirashima, S. Park, H. Sugiyama, *Chem. Commun.*, 2019, **55**, 10245-10248.

18 (a) K.-Y. Lin, R. J. Jones, M. Matteucci, *J. Am. Chem Soc.* 1995, **117**, 3873-3874; (b) J.-A. Ortega, J. R. Blas, M. Orozco, A. Grandas, E. Pedroso and J. Robles, *Org. Lett.,* 2007, **9**, 4503-4506.

19 K.-Y. Lin, M. Matteucci, *J. Am. Chem Soc.* 1998, **120**, 8531-8532.

20 (a) R. Stanton, S. Sciabola, C. Salatto, Y. Weng, D. Moshinsky, J. Little, E. Walters, J. Kreeger, D. DiMattia, T. Chen, T. Clark, M. Liu, J. Qian, M. Roy, R. Dullea, *Nucleic Acid Ther.*, 2012, **22**, 344-359; (b) W. M. Flanagan, J. J. Wolf, P. Olson, D. Grant, K.-Y. Lin, R. W. Wagner, M. D.

Matteucci, *Proc. Natl. Acad. Sci. USA.*, 1999, **96**, 3513-3518; (c) W. M. Flanagan, R. W. Wagner, D. Grant, K. -Y. Lin, M. D. Matteucci, *Nat. Biotech.*, 1999, **17**, 48-52.

21 I. Schönrath, V. B. Tsvetkov, T. S. Zatsepin, A. V. Aralov, J. Müller, *J. Biol. Inorg. Chem.,* 2019, **24**, 693-702; A. Fujii, O. Nakagawa, Y. Kishimoto, T. Okuda, Y. Nakatsuji, N. Nozaki, Y. Kasahara, S. Obika, *Chem. Eur. J.,* 2019, **25**, 7443-7448.

22 G. Stengel, M. Urban, B. W. Purse, R. D. Kuchta, *Anal. Chem.*, 2009, **81**, 9079-9085; A. M. Varizhuk, T. S. Zatsepin, A. V. Golovin, E. S. Belyaev, Y. I. Kostyukevich, V. G. Dedkov, G. A. Shipulin, G. V. Shpakovski, A. V. Aralov, *Bioorg. Med. Chem*., 2017, **25**, 3597-3605.

23 (a) Y. Kishimoto, A. Fujii, O. Nakagawa, T. Nagata, T. Yokota, Y. Hari, S. Obika, *Org. Biomol. Chem.*, 2017, **15**, 8145-8152; (b) Y. Kishimoto, O. Nakagawa, A. Fujii, K. Yoshioka, T. Nagata, T. Yokota, Y. Hari, S. Obika, *Chem. Eur. J.*, 2021, **27**, 2427-2438; (c) T. Hara, T. Kodama, Y. Takegaki, K. Morihiro, K. R. Ito, S. Obika, *J. Org. Chem.*, 2017, **82**, 25-36; (d) T. Habuchi, T. Yamaguchi, H. Aoyama, M. Horiba, K. Ito, S. Obika, *J. Org. Chem.*, 2019, **84**, 1430-1439; (e) T. Habuchi, T. Yamaguchi, S. Obika, *ChemBioChem*, 2019, **20**, 1-9.

24 (a) A. B. Eldrup, B. B. Nielsen, G. Haaima, H. Rasmussen, J. S. Kastrup, C. Christensen, P. E. Nielsen, *Eur. J. Org. Chem.,* 2001, 1781-1790; (b) A. B. Eldrup, C. Christensen, G. Haaima, P. E. Nielsen, *J. Am. Chem. Soc.,* 2002, **124**, 3254-3262.

25 C. P. Lawson, A. F. Füchtbauer, M. S. Wranne, T. Giraud, T. Floyd, B. Dumat, N. K. Andersen, A. H. El-Sagheer, T. Brown, H. Gradén, L. M. Wilhelmsson, M. Grøtli, *Sci. Rep.*, 2018, **8**, 13970.

26 D. P. Shelar, D. R. Birari, R. V. Rote, S. R. Patil, R. B. Toche, M. N. Jachak, *J. Phys. Org. Chem.,* 2011, **24**, 203-211; D. P. Shelar, S. R. Patil, R. V. Rote, R. B. Toche, M. N. Jachak, *J. Fluoresc.,* 2011, **21**, 1033-1047.

27 M. A. Cameron, S. B. Cush, R. P. Hammer, *J. Org. Chem.,* 1997, **62**, 9065-9069; T. Lan, L. W. McLaughlin, *Bioorg. Chem.,* 2001, **29**, 198-210.

28 O. Kennard, *Biochem. Soc. Trans.,* 1986, **14**, 207-210; G. Varani, W. H. McClain, *EMBO Rep.,* 2000, **1**, 18-23.

29 A. H. F. Lee, E. T. Kool, *J. Am. Chem. Soc.,* 2006, **128**, 9219-9230.

30 M. Torimura, S. Kurata, K. Yamada, T. Yakomaku, Y. Kamagata, T. Kanagawa, R. Kurane, *Anal. Sci.*, 2001, **17**, 155-160.

31 T. Maruyama, T. Shinohara, H. Ichinose, M. Kitaoka, N. Okamura, N. Kamiya, M. Goto, *Biotechnol. Lett.*, 2005, **27**, 1349-1354; M. Torimura, S. Kurata, K. Yamada, T. Yokomaku, Y. Kamagata, T. Kanagawa, R. Kurane, *Anal. Sci.*, 2001, **17**, 155-160; S. Kurata, T. Kanagawa, K. Yamada, M. Tomimura, T. Yokomaku, Y. Kamagata, R. Kurane, *Nucleic Acids Res.*, 2001, **29**, e34.

32 H. Gardarsson, A. S. Kale, S. Th. Sigurdsson, *Chembiochem*, 2011, **12**, 567-575.

33 D. Leitner, W. Schroder, K. Weisz, *Biochemistry,* 2000, **39**, 5886; A. Fujii, O. Nakagawa, Y. Kishimoto, Y. Nakatsuji, N. Nozaki, S. Obika, *ChemBioChem*, 2020, **21**, 860-864.

34 M. A. Maier, J. M. Leeds, G. Balow, R. H. Springer, R. Bharadwaj, M. Manoharan, *Biochemistry,* 2002, **41**, 1323-1327.

35 M. Meroueh, P. J. Grohar, J. Qiu, J. SantaLucia Jr, S. A. Scaringe, C. S. Chow, *Nucleic Acids Res.*, 2000, **28**, 2075-2083.